Electronic Supplementary Material (ESI) for Energy & Environmental Science.

Supplementary Information

Optimization Boosts Decarbonization: Accelerating *Net Zero* from the Perspective of Optimizing a Carbon Capture and Utilization System

Zhimian Hao,[1] Magda H. Barecka,[2] Alexei A. Lapkin[1,2*]

[1]Department of Chemical Engineering and Biotechnology, University of Cambridge, Cambridge CB3 0AS, UK

[2]Cambridge Centre for Advanced Research and Education in Singapore Ltd, 1 Create Way, CREATE Tower #05-05, 138602, Singapore

Table of Contents

S1. Rigorous process models for sub-systems

This section describes the how sub-systems are simulated in a rigorous way.

S1.1. NG-based Power plant (NGCC)

The natural gas combined cycle power plant (NGCC) is simulated in the Integrated Environmental Control Model (IECM) platform.[1] Wet cooling water is selected as the cooling system. Based on the simulation, we can obtain the consumptions of raw materials (NG, water) and emissions per unit of electricity generated.

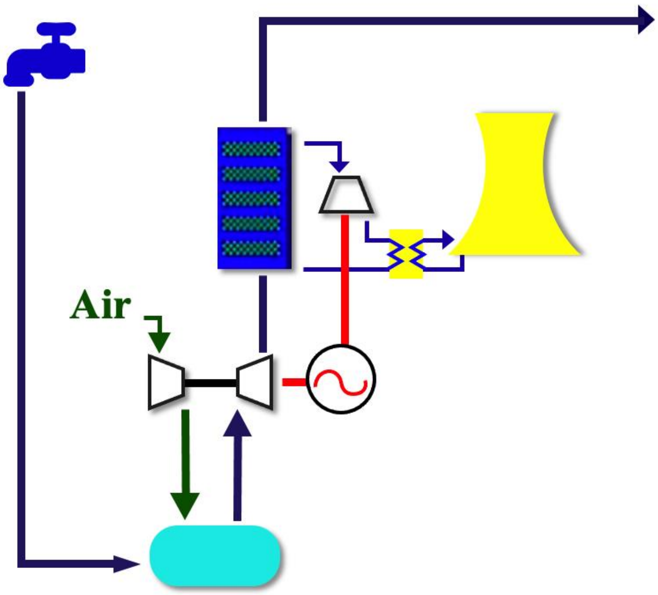

Figure S1. NGCC power plant. Reproduced from IECM.[1]

S1.2. MEA absorption process

A MEA absorption process is set up in the Integrated Environmental Control Model (IECM) platform. In IECM, a power plant equipped with carbon capture (NGCC-MEA) can be simulated. Based on the simulation, we can obtain the consumptions of raw materials (NG, water, MEA) and emissions per net electricity generated.

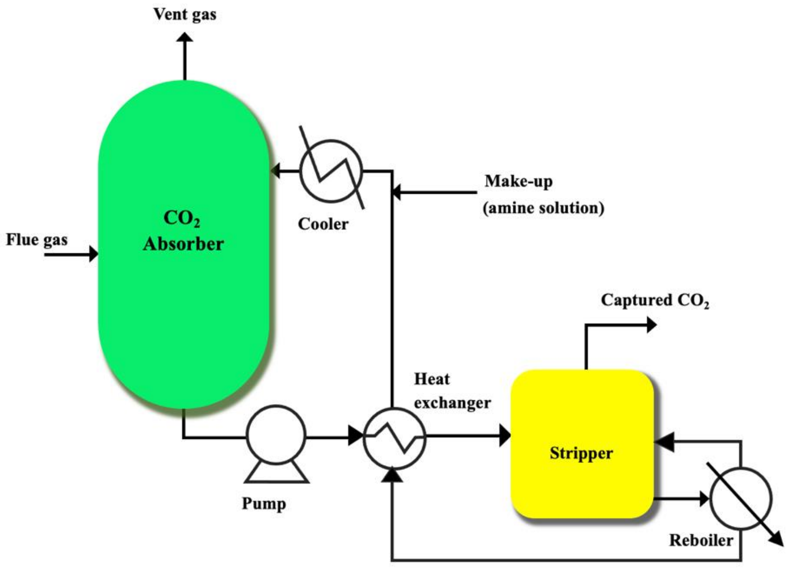

Figure S2. MEA absorption process. Reproduced from IECM.[1]

S1.3. PSA in series

A more detailed description on PSA process (balance equations, boundary conditions, cyclic steady state) can be referred to our prior work.[2] After our initial trail, one PSA unit cannot guarantee the required purity (90% for carbon capture), due to the low CO_2 concentration in the flue gas (~ 4%). Herein, we propose to use two PSA in series to gradually improve the purity of CO_2. A trade-off relationship is reported between recovery and purity.[3, 4] To maintain a relatively high recovery, the first PSA aims to increase the CO_2 purity to 20%~50% (ranging from 25% to 75% among the CO_2 purity distribution), while the second one PSA further improve the CO_2 purity over 90%.

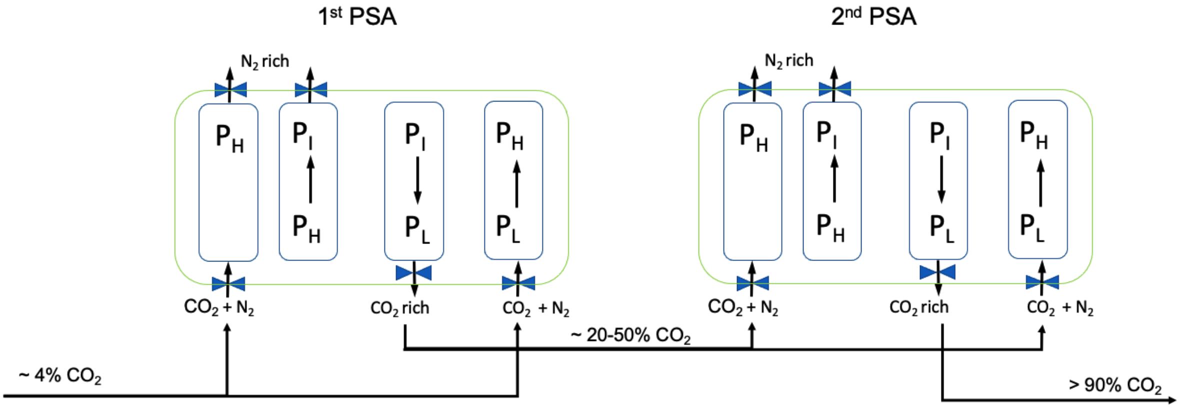

Figure S3 Two PSA in series.

S1.4. Reforming + FT

A more detailed description on [Reforming + FT] sub-system can be referred to the process modelling for GTL in our prior work.[2] This section only mentions some essential information related to this work. As shown in Figure S4, the [Reforming + FT] sub-system is modelled in Aspen Plus, including combined reforming, FT synthesis, and product upgrading section. This process starts with the combined reforming (CO_2 + H_2O) of natural gas to syngas, followed by FT synthesis for fuels. Since the upgrading section has little influence on the overall performance,[5] we use a distillation column to simplify it. To deal with a petrochemical process, Peng-Robinson is selected as the thermodynamic method.

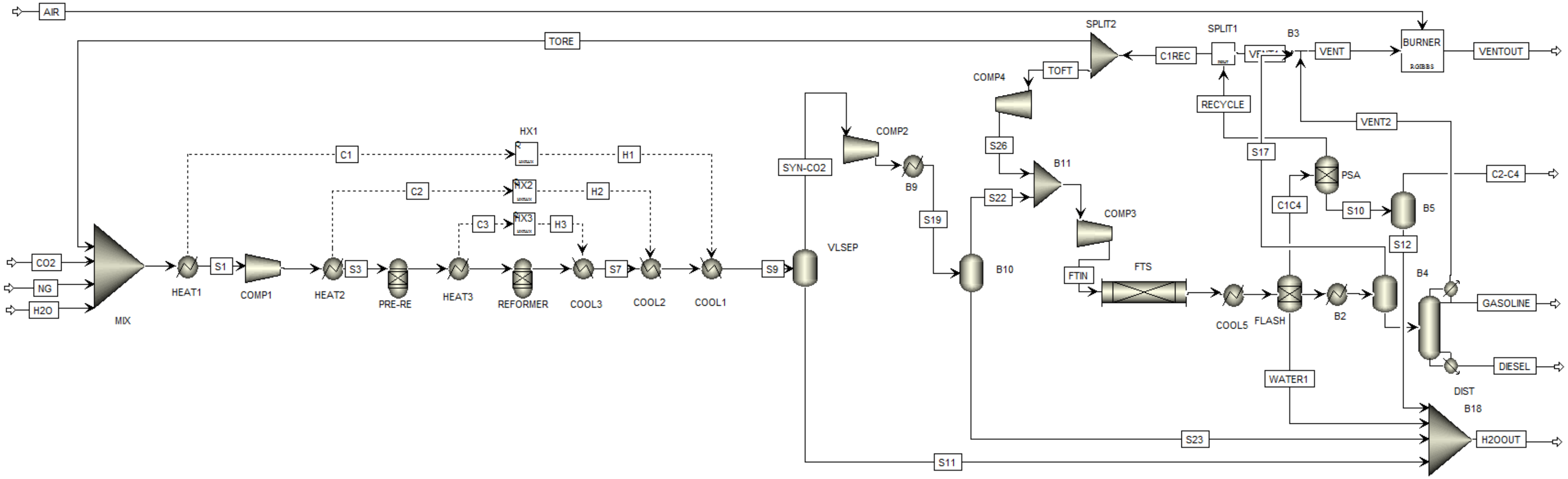

Figure S4. Flowsheet for GTL built in Aspen Plus.

S1.4.1. Combined reforming

In the reforming section, GTL starts with NG, water and CO_2. In the pre-reformer, all the carbon components are converted to CO and CH_4. In Aspen Plus, the reformer is modelled by an RGibbs reactor, where the total Gibbs energy is minimized to the reach the equilibrium ('Restricted Chemical Equilibrium' is set for the combined reforming reactions). A flowsheet option is set to vary the flowrate of H_2O and NG to guarantee the ratio of CO: H2 falls in a range of 2 – 2.2 in the reformer outlet.

Combined reforming

$$\mathrm{CH_4 + H_2O \rightarrow 3H_2 + CO}$$

$$\mathrm{CH_4 + CO_2 \rightarrow 2H_2 + 2CO}$$

S1.4.2. Fischer-Tropsch

Fischer-Tropsch (FT) has a long industrial history of producing high-quality fuels.[6, 7] Low-temperature FT (LTFT) is considered in this work. This is because FT reaction is highly exothermic, and a lower temperature can improve the final conversion regarding the thermodynamic equilibrium. For LTFT, the desired syngas ratio falls in the range of 2 – 2.2 for H_2 : CO,[5-7] and the reaction temperature is reported to range from 200 to 270 °C [6, 8, 9] as well as pressure in 15 – 50 bar.[8-10]

$$\mathrm{(2n + 1)H_2 + nCO \rightarrow C_nH_{2n+2} + nH_2O}$$

For FT kinetics, Yates et al. developed a simple but reliable expression 30 years ago for the consumption rate of CO as Equation S.1.[11]

$$\mathrm{r_{CO} = \frac{F \cdot a \cdot P_{CO} \cdot P_{H_2}}{(1 + b \cdot P_{CO})^2}} \tag{S.1}$$

where, F: catalyst improvement factor since Yates' kinetics proposed in 1991;

P_i: partial pressure of component i;

a: reaction rate coefficient;

b: adsorption coefficient.

In the FT section, the syngas is pressurized before entering the FT reactor. RPlug is chose to simulate the multi-tubular fixed-bed reactor for FT in Aspen Plus. Yates' kinetics is used for the overall consuming rate of CO (r_{CO}),[11] while the Anderson-Schulz-Flory mechanism can be used to estimate the distribution of FT products.[7] Since the properties of hydrocarbons (HCs) are similar, .we employ four reactions (R1~R4) to represent the whole range of HCs for simplification during the simulation as the Table S1. CO_2 is reported not to react on the Cobalt-based catalyst and can be regarded as an inert gas in the FT reaction.[12, 13] Based on the information mentioned above, we used the kinetic information in Rplug model.

Table S1. Components and reactions used in the simulation.

C range	Molar fraction	Representations	Representative reactions	R_{CO}
C_1	0.07	CH_4	R1: $3H_2 + CO \rightarrow CH_4 + H_2O$	$0.007r_{CO}$
$C_2\sim C_4$	0.18	C_3H_8	R2: $7H_2 + 3CO \rightarrow C_3H_8 + 3H_2O$	$0.053r_{CO}$
$C_5\sim C_{12}$	0.30	C_8H_{18} (gasoline)	R3: $17H_2 + 8CO \rightarrow C_8H_{18} + 8H_2O$	$0.234r_{CO}$
C_{13+}	0.45	$C_{16}H_{34}$ (diesel)	R4: $33H_2 + 16CO \rightarrow C_{16}H_{34} + 16H_2O$	$0.706r_{CO}$
Total	1.00			r_{CO}

S1.4.3. Separation and recovery

Following the FT reactor, a three-phase flash is used to split the mixed stream into gas, liquid HCs and wastewater. As a simplification to the upgrading system, we use a distillation column (RadFrac) to separate gasoline from diesel. For the gas mixture in the simulation, we use an ideal separator (in the real world, PSA can be an option) to recycle all the C1 components. The GTL system contains inert gas (N_2), which must be purged (otherwise, it will gradually accumulate in the recycle stream, making the convergence impossible to achieve). Herein, the recycle stream is split to *vent* (to purge) and *C1REC*, which will be followed by splitting into reforming section and FT sections, respectively.

S1.4.4. Utility and its integration

The heating utility is supplied by steam at 300 °C and fuel gas over 1000 °C. The cooling utility is provided by air and cooling water at room temperature. Pump and compressor are powered by electricity.

A high temperature is required for the reforming reaction. Thus, the reformer outflow has an extremely high temperature and needs to be cooled before the FT process. We built three heat exchangers to gradually cool down the reformer outflow, while the recycled heat is used to preheat the mixed stream to the gas form (>100 ℃), an intermediate temperature for pre-reformer (~ 500 ℃) and a high temperature for reformer (700 ~ 1000 ℃).

Additionally, the purge stream contains CO and CH_4, which will bring in considerable greenhouse emissions if the direct emissions apply. With the assistance of air, a burner is used to deal with these C1 components. An RGibbs reactor @ 600 ℃ is used to simulate the burner. Due to the exothermic reactions, the burner will release heat, while the waste heat recovery technology[14, 15] can be used to recover the part of burner heating (utilization efficiency is assumed at $\eta_{burner} = 60\%$) to reduce the heating utility of steam or fuel gas.

S1.5. Reforming + MS

The [Reforming + MS] sub-system contains two sections: (1) combined reforming, which generates the syngas with the composition ratio as $\frac{2CO+3CO_2}{H_2} = 1$ (Figure S5); (2) methanol synthesis (MS) converted the syngas to methanol (Figure S6). The MS process model was reported in the Aspen Plus model library.[16]

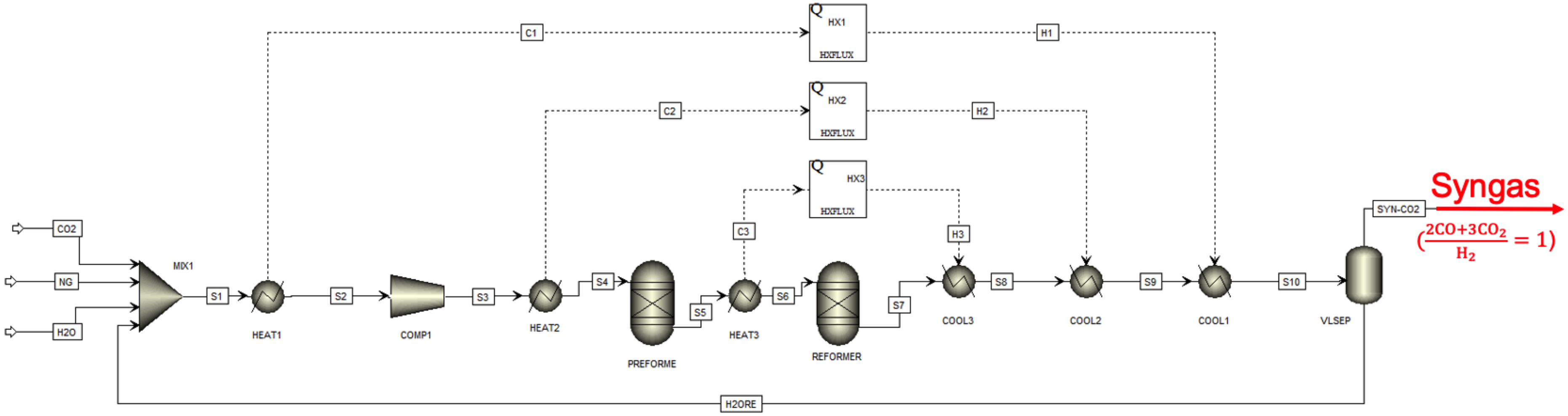

Figure S5. Reforming section for [Reforming + MS].

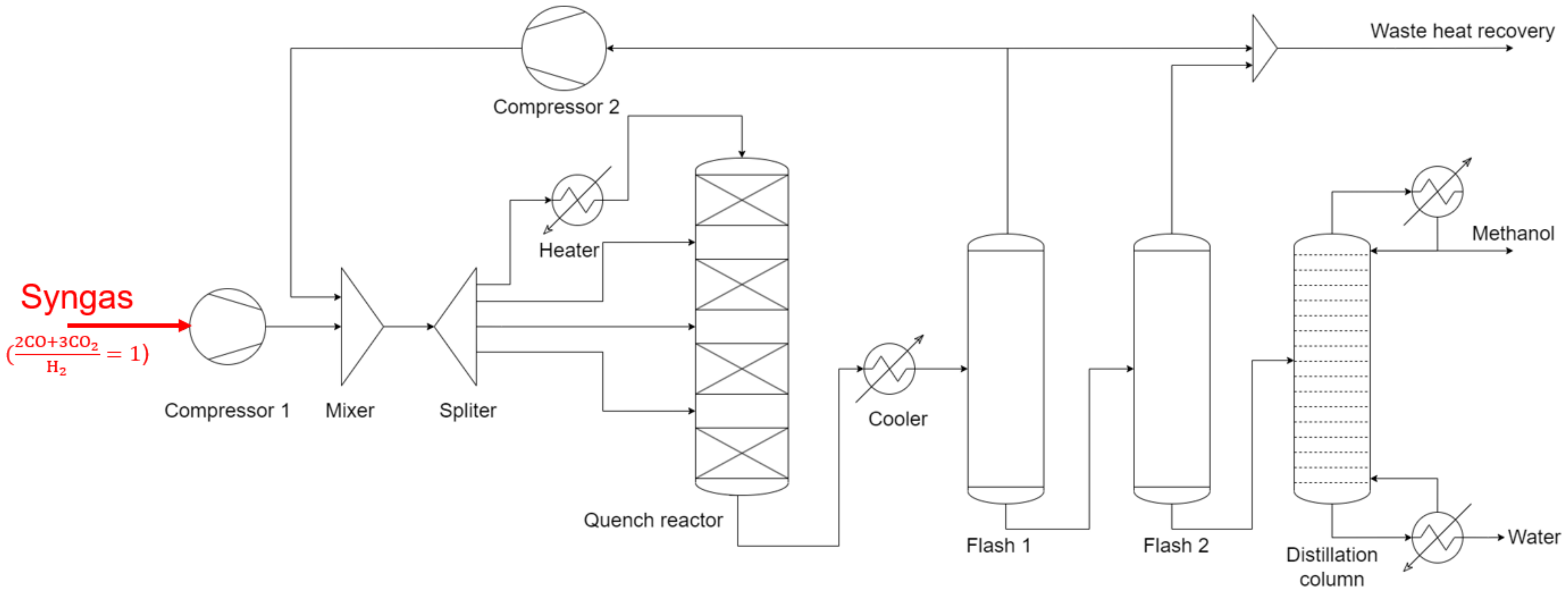

Figure S6. A simplified process flow diagram for MS process, which is based on Aspen Tech model library.[16]

S1.5.1. Combined reforming

Combined reforming section is similar to S1.4.1. Combined reforming ; flowsheet options are set to manipulate the flowrates of NG and inlet water, in order to the guarantee the optimal syngas ratio as $\frac{2CO+3CO_2}{H_2}=1$ for MS reaction (Figure S5)

S1.5.2. Methanol synthesis

For the MS section, Aspen Tech Model library offers an industrial-scale process model (Figure S6), where the thermodynamics, reaction kinetics and mass balance are validated. The process model is reported to be capable to simulate an industrial methanol process - ICI Synetix low pressure methanol process (LPM). A four-stage quench reactor is used to perform the heat integration between the inlet stream and exothermic MS reactions. More detailed information about the process models can be referred to the Aspen Tech documents.[16]

$$CO_2 + 3H_2 \leftrightarrow CH_3OH + H_2O$$

$$CO_2 + H_2 \leftrightarrow CO + H_2O \text{ (RWGS)}$$

Vanden Bussche and Froment kinetics[17] are used for MS.

$$r_{MS} = \frac{k_{MS} p_{CO_2} p_{H_2} \left(1 - \frac{p_{CH_3OH} p_{H_2O}}{K_{MS} p_{H_2}^3 p_{CO_2}}\right)}{\left(1 + K_A \frac{p_{H_2O}}{p_{H_2}} + K_B p_{H_2}^{0.5} + K_C p_{H_2O}\right)^3} (W_{cat} F_{cat}) \tag{S.2}$$

$$r_{RWGS} = \frac{k_{RWGS} p_{CO_2} \left(1 - \frac{p_{CO} p_{H_2O}}{K_{RWGS} p_{CO_2} p_{H_2}}\right)}{\left(1 + K_A \frac{p_{H_2O}}{p_{H_2}} + K_B p_{H_2}^{0.5} + K_C p_{H_2O}\right)} (W_{cat} F_{cat}) \tag{S.3}$$

Where the rate constants can be expressed as follows,

$$k_{MS} = k_{MS,ref} \exp\left(-\frac{E_{MS}}{R}\left(\frac{1}{T} - \frac{1}{T_{ref}}\right)\right) \tag{S.4}$$

$$k_{RWGS} = k_{RWGS,ref} \exp\left(-\frac{E_{RWGS}}{R}\left(\frac{1}{T} - \frac{1}{T_{ref}}\right)\right) \tag{S.5}$$

where, r_{MS}: rate of methanol synthesis, kmol/s;

p_i: partial pressure of component i, bar ($i = H_2, H_2O, CH_3OH, CO, CO_2$);

k_j: rate constant of reaction j, kmol/kg-cat/s ($j = MS, RWGS$)

T_{ref}: reference temperature, 501.57 K

$k_{j,ref}$: rate constant of reaction j @ T_{ref}, kmol/kg-cat/s ($j = MS, RWGS$)

E_j: activation energy of reaction j, kmol/kg-cat/s ($j = MS, RWGS$)

K_j: equilibrium constant of reaction j ($j = MS, RWGS$), expressed as $\ln K_j = A_j + \frac{B_j}{T}$

W_{cat}: rate constant of reaction j, kmol/kg-cat/s ($j = MS, RWGS$)

F_{cat}: catalyst activity factor, F_{cat}=1 @ fresh catalyst.

S1.5.3. Separation and recovery

We do not modify the separation part of the original process model. More detailed information about the process models can be referred to the Aspen Tech documents.[16]

S1.5.4. Utility and its integration

This section is the same as the Section S1.4.4. Utility and its integration.

S2. Overview of essential input/output of sub-systems

The carbon capture and utilization (CCU) system can be divided into four sub-systems: [NGCC + MEA], [NGCC + PSA], [Reforming + FT] and [Reforming + MS]. Table S2 lists the input and output for sub-systems. The input of a sub-system contains the decision variables and relevant variables from other sub-system. The output of a sub-system contains its mass and energy balance. After the decision variables $\theta = [\theta_{MEA}, \theta_{PSA1}, \theta_{PSA2}, z_{FT}, \theta_{FT}, \theta_{MS}, \epsilon, \varepsilon]$ are given a set of values, the mass and energy balance of the whole CCU system can be assembled from the sub-systems.

Table S2. Inputs and outputs for sub-systems.

Sub-systems (i)	Input	Output
NGCC + MEA	θ_{MEA}	$F_{MEA,CO_2cap}, F_{MEA,CO_2e}, E_{NGCC-MEA}$
NGCC + PSA	$[\theta_{PSA1}, \theta_{PSA2}]$	$F_{PSA,CO_2cap}, F_{PSA,CO_2e}, E_{NGCC-PSA}$
Reforming + FT	$[\theta_{FT}, F_{MEA,CO_2cap}, F_{PSA,CO_2cap}, z_{FT}]$	$F_{FT,r}, F_{FT,p}, F_{FT,CO_{2e}}, U_{FT,u}$
Reforming + MS	$[\theta_{MS}, F_{MEA,CO_2cap}, F_{PSA,CO_2cap}, 1 - z_{FT}]$	$F_{MS,r}, F_{MS,p}, F_{MS,CO_{2e}}, U_{MS,u}$

Where,

θ_{MEA}: decision variables for MEA absorption process.

θ_{PSA1}: decision variables for 1st PSA process.

θ_{PSA2}: decision variables for 2nd PSA process.

θ_{FT}: decision variables for [reforming + FT].

θ_{MS}: decision variables for [reforming + MS] sub-system.

z_{FT}: distribution of captured CO_2 to FT process.

F_{MEA,CO_2cap}: mass flow of captured CO_2 by MEA absorption process, ton_{CO_2}/h.

F_{MEA,CO_2e}: mass flow of uncaptured CO_2 by MEA absorption process, ton_{CO_2}/h.

F_{PSA,CO_2cap}: mass flow of captured CO_2 by the two PSA in series, ton_{CO_2}/h.

F_{PSA,CO_2e}: mass flow of uncaptured CO_2 by the two PSA in series, ton_{CO_2}/h.

$E_{NGCC-MEA}$: net electricity output for [NGCC + MEA] sub-system, netMW.

$E_{NGCC-PSA}$: net electricity output for [NGCC + PSA] sub-system, netMW.

$F_{ii,r}$: mass flow for required raw materials, $ii = [FT, MS], r = [NG, H_2O]$, ton/h.

$F_{ii,p}$: mass flow for products, $ii = [FT, MS], p = [gasoline, diesel, MEOH]$, ton/h.

F_{ii,CO_2e}: mass flow for CO_2 emissions via the vent gas, $ii = [FT, MS]$, ton/h.

$U_{ii,u}$: utility consumption, $ii = [FT, MS], u = [fuel\ gas, steam, electricity, cooling]$, GJ/h.

S3. Surrogates for sub-systems

S3.1. NGCC

There is no surrogate here. For NGCC, the IECM software can yield

GHG_{MWh}: emissions per unit of electricity generation, ton/MWh;

NG_{MWh}: NG consumption per unit of electricity generation, ton/MWh;

H_2O_{MWh}: water consumption per unit of electricity generation, ton/MWh.

S3.2. [NGCC + MEA]

The [NGCC + MEA] sub-system aims to build the relationship between θ_{MEA} and $[F_{MEA,CO_2cap}, F_{MEA,CO_2e}, E_{NGCC-MEA}]$.

θ_{MEA} only contains one decision variable as the recovery rate of CO_2 in MEA process $(Re_{CO_2,MEA})$. When assigning a set of values to Re_{MEA}, the IECM software can yield the corresponding simulation outputs. With the inputs/outputs, we train a linear regression model as follows:

$$[Re_{MEA}, \eta_{MEA}, H_2O_{netMWh}, MEA_{netMWh}] = surrogate_{NGCC-MEA}(\theta_{MEA}) \qquad S.6$$

Where, Re_{MEA}: recovery rate of CO_2 in MEA process.

η_{MEA}: net power out per NGCC power generation (partial loss in MEA), netMW/MW

After coupled with a MEA absorption process, a 500 MW NGCC power station generate net power ($E_{NGCC-MEA}$, netMW) and captured CO_2 (F_{MEA,CO_2cap}, ton_{CO_2}/h) as follows,

$$E_{NGCC-MEA} = \eta_{MEA} \cdot 500 \qquad S.7$$

$$F_{MEA,CO_2cap} = 500 \cdot GHG_{MWh} \cdot Re_{MEA} \tag{S.8}$$

$$F_{MEA,CO_2e} = 500 \cdot GHG_{MWh} \cdot (1 - Re_{MEA}) \tag{S.9}$$

S3.3 [NGCC + PSA]

The [NGCC + MEA] sub-system aims to build the relationship between $[\theta_{PSA1}, \theta_{PSA2}]$ and $[F_{PSA,CO_2cap}, F_{PSA,CO_2e}, E_{NGCC-PSA}]$.

Two surrogates are built for two PSA processes, respectively. The obtained CO_2 purity from 1st PSA is the inlet CO_2 concentration for the 2nd PSA. Their input variables are as follows,

$$\theta_{PSA1} = [P_{L1}, P_{I1}, v_{feed1}, t_{ads1}, t_{bd1}, t_{evac1}]$$

$$[Pu_{PSA1}, \theta_{PSA2}] = [Pu_{PSA1}, P_{L2}, P_{I2}, v_{feed2}, t_{ads2}, t_{bd2}, t_{evac2}]$$

A well-distributed values for input can generated by employing Latin hypercube sampling (LHS) for the design space of input variables. Based on these input values, the rigorous PSA simulation on Dymola can yield outputs (purity, recovery and energy consumption). With the inputs/outputs, we train two ANN models as follows,

$$[Pu_{PSA1}, Re_{PSA1}, Energy_{PSA1}] = Surrogate_{PSA1}(\theta_{PSA1}) \tag{S.10}$$

$$[Pu_{PSA2}, Re_{PSA2}, Energy_{PSA2}] = Surrogate_{PSA2}([Pu_{PSA1}, \theta_{PSA1}]) \tag{S.11}$$

Where, Re_{PSA1}: recovery rate of CO_2 in 1st PSA process

Re_{PSA1}: recovery rate of CO_2 in 2nd PSA process

$Energy_{PSA1}$: energy consumption per CO_2 captured in 1st PSA, MWh/ton_{CO_2}

$Energy_{PSA2}$: energy consumption per CO_2 captured in 2nd PSA, MWh/ton_{CO_2}.

The overall performance for [NGCC + PSA] sub-system can be obtained in the following equations:

$$Pu_{PSA} = Pu_{PSA2} \tag{S.12}$$

$$Re_{PSA} = Re_{PSA1} \cdot Re_{PSA2} \tag{S.13}$$

$$\eta_{PSA} = 1 - GHG_{MWh} \cdot (Energy_{PSA1} \cdot Re_{PSA1} + Energy_{PSA2} \cdot Re_{PSA}) \tag{S.14}$$

Where Pu_{PSA}: purity of CO_2 from the two PSA

Re_{PSA}: recovery rate of CO_2 from the two PSA

η_{PSA}: net power out per NGCC power generation (partial loss in PSA), netMW/MW

After coupled with two PSA in series, a 500 MW NGCC power station generate net power ($E_{NGCC-PSA}$, netMW) and captured CO2 (F_{PSA,CO_2cap}, ton_{CO_2}/h) as follows,

$$E_{NGCC-MEA} = \eta_{PSA} \cdot 500 \tag{S.15}$$

$$F_{PSA,CO_2cap} = 500 \cdot GHG_{MWh} \cdot Re_{PSA} \tag{S.16}$$

$$F_{PSA,CO_2e} = 500 \cdot GHG_{MWh} \cdot (1 - Re_{PSA}) \tag{S.17}$$

S3.4. Reforming + FT

The [Reforming + FT] sub-system aims to build the relationship between $[\theta_{FT}, F_{MEA,CO_2cap}, F_{PSA,CO_2cap}, z_{FT}, \epsilon, \varepsilon]$ and $[F_{FT,r}, F_{FT,p}, F_{FT,CO_{2e}}, U_{FT,u}]$.

The amount of CO2 flowing to [Reforming + FT] can be calculated as follows,

$$F_{FT,CO_2} = (F_{MEA,CO_2cap} + F_{PSA,CO_2cap}) \cdot z_{FT} \tag{S.18}$$

The input variables for [Reforming + FT] are as follows,

$$[F_{FT,CO_2}, \theta_{FT}] = [F_{FT,CO_2}, T_{FT}, P_{FT}, Tray_{ref1}, T_{ref1}, P_{ref1}, S_{purge}, Re_{FT}]$$

A well-distributed values for input can generated by employing Latin hypercube sampling (LHS) for the design space of input variables. Based on these input values, the rigorous simulation on Aspen Plus can yield outputs (mass flows and utilities). With the inputs/outputs, we train an ANN model for [Reforming + FT] sub-system as follows,

$$[F_{FT,r}, F_{FT,p}, F_{FT,CO_{2e}}, U_{FT,u}] = Surrogate_{reforming+FT}([F_{FT,CO_2}, \theta_{FT}]) \tag{S.19}$$

S3.5. Reforming + MS

The [Reforming + MS] sub-system aims to build the relationship between $[\theta_{MS}, F_{MEA,CO_2cap}, F_{PSA,CO_2cap}, 1 - z_{FT}]$ and $[F_{MS,r}, F_{MS,p}, F_{MS,CO_{2e}}, U_{MS,u}]$.

The amount of CO2 flowing to [Reforming + MS] can be calculated as follows,

$$F_{MS,CO_2} = (F_{MEA,CO_2cap} + F_{PSA,CO_2cap}) \cdot (1 - z_{FT}) \tag{S.20}$$

The input variables for [Reforming + MS] are as follows,

$$[F_{MS,CO_2}, \theta_{MS}] = [F_{MS,CO_2}, T_{FT}, P_{FT}, Tray_{ref1}, T_{ref1}, P_{ref1}, S_{purge}, Re_{FT}]$$

A well-distributed values for input can generated by employing Latin hypercube sampling (LHS) for the design space of input variables. Based on these input values, the rigorous simulation on Aspen Plus can yield outputs (mass flows and utilities). With the inputs/outputs, we train an ANN model for [Reforming + MS] sub-system as follows,

$$[\mathrm{F_{MS,r}}, \mathrm{F_{MS,p}}, \mathrm{F_{MS,CO_{2e}}}, \mathrm{U_{MS,u}}] = \mathrm{Surrogate_{reforming+MS}}([\mathrm{F_{MS,CO_2}}, \theta_{\mathrm{MS}}]) \qquad \text{S.21}$$

S4. Evaluation of GHG emissions for the industrial park

S4.1. System boundary in this work: cradle-to-gate

This section explains the 'cradle-to-gate' boundary adopted for the analysis. The GHG emissions for the whole CCU system are evaluated based on the life cycle assessment (LCA). The system boundary determines the life cycle stages required for the evaluation. A strict LCA can cover the evaluation of emissions throughout entire 'cradle-to-grave' life cycle stages ranging from raw material, manufacturing, distributing, use, to recycling/disposal. However, the evaluation of the entire life cycle of a product requires excessive workloads. Further, LCA is mainly used in comparative assessments. The cradle-to-gate (from raw materials to manufacturing) is sufficient to compare the emissions for different technology, while the downstream emissions are identical.[18] As shown in Figure S7, the cradle-to-gate approach for the CCU system will quantify the GHG emissions of raw materials and utility as well as CO_2 emissions in the process (*e.g.* uncaptured CO_2 and CO_2 emissions via vent gas).

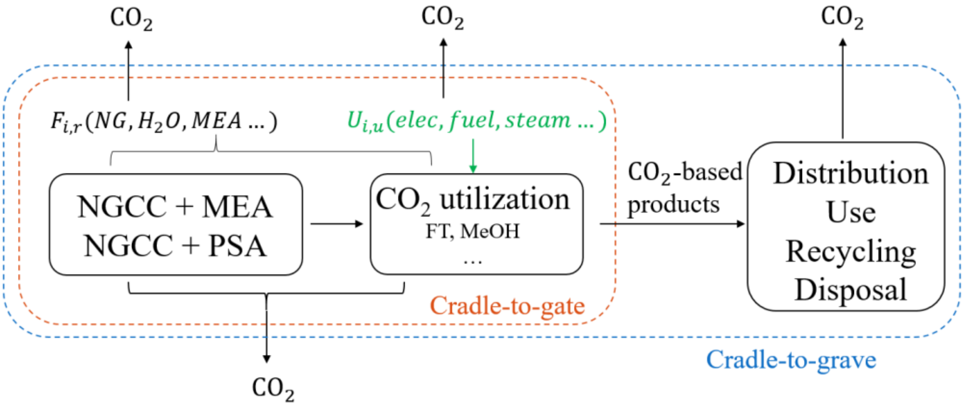

Figure S7. System boundaries of cradle-to-gate vs. cradle-to-grave approach for the emissions of a CCU system.

S4.2. System expansion strategy to compare CCU with a reference process.

The 'system expansion' strategy is particularly useful for LCA of a system with multiple functions.[18] The CCU system achieves multiple functions, i.e. the co-productions of several fuels and the generation of low-carbon electricity. For a proper comparison, the 'system expansion' strategy expands a reference process to include all the functions as the original process. As shown in Figure S8, the reference system can generate the electricity (no capture technology) and fuels by conventional process. Meanwhile, the amount of electricity generation and the production of fuels are equivalent in the two systems for a fair comparison.

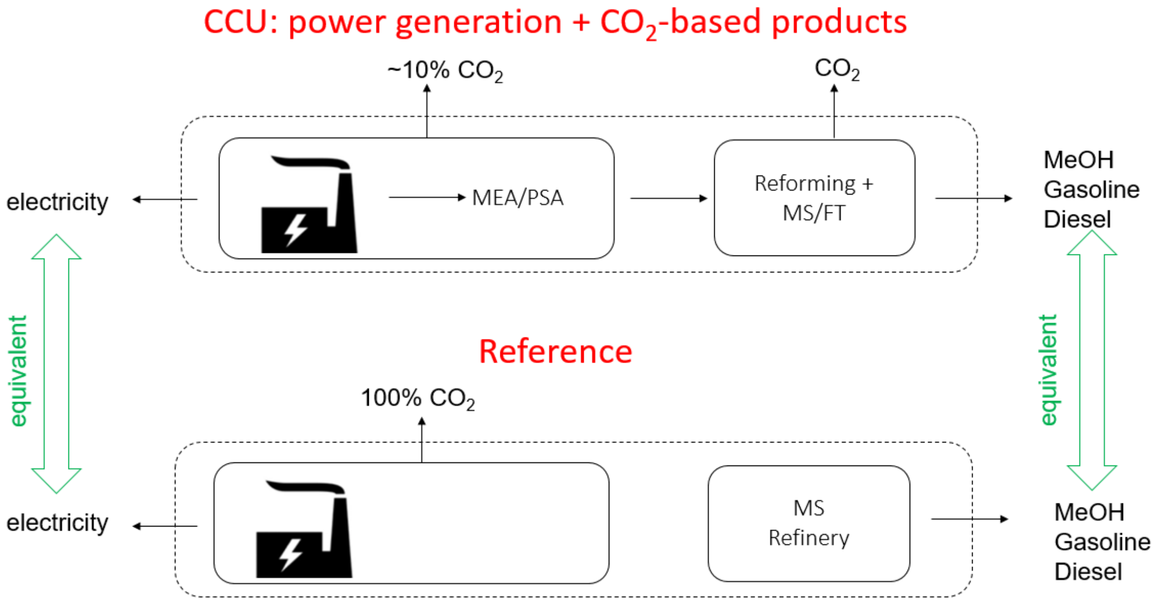

Figure S8. Expansion strategy for a fair comparison between CCU system and a conventional system.

S4.3. The reduction of GHG emissions

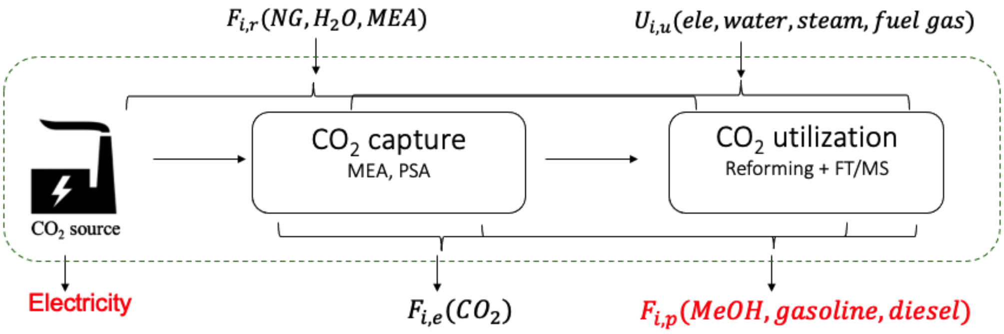

Figure S9. Sources of GHG emissions in the cradle-to-gate system boundary.

$$\mathrm{GHG_{CCU}} = \sum_{i}\sum_{r} \alpha_r \cdot F_{i,r} + \sum_{i}\sum_{u} \alpha_u \cdot U_{i,u} + \sum_{i} F_{i,CO2} \qquad S.22$$

$$\mathrm{GHG_{ref}} = \alpha_{NGCC} \cdot E_{electricity} + \sum_{i}\sum_{p} \alpha_p \cdot F_{i,p} \qquad S.23$$

$$\mathrm{GHG_{reduction}} = 1 - \frac{\mathrm{GHG_{CCU}}}{\mathrm{GHG_{ref}}} \qquad S.24$$

Where

F: mass flow, ton/hour

U: utility, GJ/hour

α_r: emission factor per raw material r generation: $\mathrm{ton_{CO_2eq}/ton_r}$

α_u: emission factor per utility u generation: $\mathrm{ton_{CO_2eq}/GJ}$

α_p: emission factor per product p generation: $\mathrm{ton_{CO_2eq}/ton_p}$

Subscript

i: notation for sub-systems

r: notation for raw materials (natural gas, process water, MEA)

u: notation for utilities (steam, fuel gas, electricity, cooling water)

p: notation for products

S4.4. Calculation of emission factors for low-carbon electricity

In this work, the emission factor is defined as the GHG emission in generating a material (per ton) or a utility (per GJ). In the proposed industrial park, two 500 MW power stations generate electricity by natural gas combined cycle (NGCC) technology. When no carbon capture is applied, as shown in Equation S.*25*, the emission factor per unit of electricity generation is calculated by the sum of emissions in generating raw materials (NG, water) together with the direct emissions. As such, the emission factor of NGCC electricity is calculated as 0.41 $\mathrm{kg_{CO_2eq}/kWh}$, which falls in the range reported by Weisser.[19]

$$\alpha_{NGCC} = \frac{\sum_r \alpha_r \cdot F_{NGCC,r} + F_{NGCC,CO_2e}}{E_{NGCC}} \qquad S.25$$

In our work, the low-carbon electricity specifically refers to CCS electricity (NGCC integrated with CCS). MEA decarbonizes one NGCC, while PSA decarbonizes the other one. The emission factors of low-carbon electricity is approximated by the average value between [NGCC-PSA-storage] and [NGCC-MEA-storage]. Equation S.*26*-S.*28* shows how the emission factor for low-carbon electricity. As such, the cost of low-carbon electricity is estimated at 0.098 $\mathrm{kg_{CO_2}/kwh}$ (value may slightly change subject to the amount of CO_2 captured), which is in agreement with the literature value.[19]

$$\alpha_{CCS} = (\alpha_{PSA} + \alpha_{MEA})/2 \qquad S.26$$

$$\alpha_{PSA} = \frac{\sum_r \alpha_r \cdot F_{NGCC,r} + F_{PSA,CO_2e}}{E_{NGCC-PSA}} \qquad S.27$$

$$\alpha_{MEA} = \frac{\sum_r \alpha_r \cdot F_{NGCC,r} + \sum_r \alpha_r \cdot F_{MEA,r} + F_{MEA,CO_2e}}{E_{NGCC-MEA}} \qquad S.28$$

E_{NGCC}: power generation of NGCC, GJ/h

$E_{NGCC-PSA}$: net power out for a NGCC coupled with PSA, GJ/h

$E_{NGCC-MEA}$: net power out for a NGCC coupled with MEA, GJ/h

F_{PSA,CO_2e}: emissions for a NGCC coupled with PSA, $\mathrm{ton_{CO_2}/h}$

F_{MEA,CO_2e}: emissions for a NGCC coupled with MEA, $\mathrm{ton_{CO_2}/h}$

F_{PSA,CO_2s}: the amount of stored CO_2 for a NGCC coupled with PSA, $\mathrm{ton_{CO_2}/h}$

F_{MEA,CO_2s}: the amount of stored CO_2 for a NGCC coupled with MEA, $\mathrm{ton_{CO_2}/h}$

$F_{MEA,r}$: mass flow of raw materials (MEA, H_2O) in MEA absorption process, ton/hour

Subscript:

CO_{2e}, CO_2 emission to envrioment

CO_{2s}, CO_2 storage to underground

S4.5. Calculation of GHG emission factor for low-carbon heating

In this work, heating is proposed to be partially substituted by CCS electricity. As such, low-carbon heating is used in the CCU system. Herein, the GHG emission factor for low-carbon heating is calculated as follows,

$$\alpha_{\mathrm{fuel}_{\mathrm{low-C}}} = \epsilon \cdot \alpha_{\mathrm{CCS}} + (1-\epsilon)\alpha_{\mathrm{fuel}} \qquad \text{S.29}$$

$$\alpha_{\mathrm{steam}_{\mathrm{low-C}}} = \varepsilon \cdot \alpha_{\mathrm{CCS}} + (1-\varepsilon)\alpha_{\mathrm{steam}} \qquad \text{S.30}$$

Where,

$\alpha_{\mathrm{fuel}_{\mathrm{low-C}}}$: GHG emission factor for low-carbon heating (partially by CCS electricity and partially by fuel gas), ton/GJ

α_{fuel}: GHG emission factor for heating by fuel gas, ton/GJ

$\alpha_{\mathrm{steam}_{\mathrm{low-C}}}$: GHG emission factor for low-carbon heating (partially by CCS electricity and partially by steam), ton/GJ

α_{steam}: GHG emission factor for heating by steam, ton/GJ

S4.6. Data for GHG emissions factors

α_{r}: emission factor per raw material r generation: $\mathrm{ton}_{\mathrm{CO_2eq}}/\mathrm{ton}_{\mathrm{r}}$

α_{u}: emission factor per utility u generation: $\mathrm{ton}_{\mathrm{CO_2eq}}/\mathrm{GJ}$

α_{p} : emission factor per product p generation (in conventional or reference process): $\mathrm{ton}_{\mathrm{CO_2eq}}/\mathrm{ton}_{\mathrm{p}}$

Table S3. GHG emissions factors for materials (α_r or α_p) and utilities (α_u)

	GHG emissions factors	Unit	source
Natural gas	0.354	$\mathrm{ton}_{\mathrm{CO_2eq}}/\mathrm{ton}_{\mathrm{NG}}$	1)
Process water	5.4e-4	$\mathrm{ton}_{\mathrm{CO_2eq}}/\mathrm{ton}_{\mathrm{water}}$	1)
Methanol	0.762	$\mathrm{ton}_{\mathrm{CO_2eq}}/\mathrm{ton}_{\mathrm{MEOH}}$	1)
Gasoline	0.802	$\mathrm{ton}_{\mathrm{CO_2eq}}/\mathrm{ton}_{\mathrm{gasoline}}$	1)
Diesel	0.663	$\mathrm{ton}_{\mathrm{CO_2eq}}/\mathrm{ton}_{\mathrm{diesel}}$	1)
MEA	3.40	$\mathrm{ton}_{\mathrm{CO_2eq}}/\mathrm{ton}_{\mathrm{MEA}}$	2)
Ethanol	3.74	$\mathrm{ton}_{\mathrm{CO_2eq}}/\mathrm{ton}_{\mathrm{EtOH}}$	3)
C2-C4	1.11	$\mathrm{ton}_{\mathrm{CO_2eq}}/\mathrm{ton}_{\mathrm{C3}}$	4)

Electricity	0.114	$\mathrm{ton_{CO_2eq}/GJ_{NGCC}}$	5)
Fuel gas	0.079	$\mathrm{ton_{CO_2eq}/GJ_{fuel-gas}}$	1)
Steam	0.083	$\mathrm{ton_{CO_2eq}/GJ_{steam}}$	1)
Cooling water	8.04e-3	$\mathrm{ton_{CO_2eq}/GJ_{cooling}}$	6)

1) Roh et al.[20]
2) Cuéllar-Franca et al.[21]
3) Munoz et al.[22]
4) Average the emission factors of propene and propane in the software Umberto (method: ReCiPe Midpoint (H) w/o LT).
5) The emission factor of electricity (from a NGCC power plant) is based on the sum of NG, process water, CO_2 emissions (refer to Equation S.25).
6) The emission factor of cooling is calculated by water emission factor times its required amount (based on $\Delta T = 20°C$, heat transfer efficiency $\eta = 0.8$).

S5. Evaluation of economic aspect for the industrial park

S5.1. The calculation of profits

$$\mathrm{Profit_{CCU}} = -\sum_{i}\sum_{r}\beta_r \cdot F_{i,r} - \sum_{i}\sum_{u}\beta_u \cdot U_{i,u} - \sum_{i} F_{i,CO2} \cdot \gamma_{CO_2} + \beta_{CCS} \cdot E_{electricity} + \sum_{i}\sum_{p}\beta_p \cdot F_{i,p} \qquad \text{S.31}$$

Where

F: mass flow, ton/hour

U: utility, GJ/hour

β_r: cost of raw material r, \$/ton

β_u: cost of utility u, \$/GJ

γ_{CO_2}: carbon tax (carbon price), \$/$\mathrm{ton_{CO_2}}$

β_{CCS}: cost of low-carbon electricity (equivalent to CCS electricity), \$/GJ

β_p: price of product p, \$/ton

Subscript

i: notation for sub-systems

r: notation for raw materials (natural gas, process water, MEA)

u: notation for utilities (steam, fuel gas, electricity, cooling water)

p: notation for products

S5.2. Calculation of economic factors for low-carbon electricity

Economic factors refer to the costs of raw materials and utilities as well as the prices of products. The emission factors of low-carbon electricity is approximated by the average value between [NGCC-PSA-storage] and [NGCC-MEA-storage]. The cost of carbon storage is obtained by IECM software.

$$\mathrm{\beta_{CCS} = (\beta_{PSA} + \beta_{MEA})/2} \qquad \text{S.32}$$

$$\mathrm{\beta_{PSA}} = \frac{\mathrm{\beta_{NGCC} \cdot E_{NGCC} + \gamma_{CO_2} \cdot F_{PSA,CO_2e} + \delta_{CO_2} \cdot F_{PSA,CO_2s}}}{\mathrm{E_{NGCC-PSA}}} \qquad \text{S.33}$$

$$\mathrm{\beta_{MEA}} = \frac{\mathrm{\beta_{NGCC} \cdot E_{NGCC} + \sum_r \ \beta_r \cdot F_{MEA,r} + \gamma_{CO_2} \cdot F_{MEA,CO_2e} + \delta_{CO_2} \cdot F_{MEA,CO_2s}}}{\mathrm{E_{NGCC-MEA}}} \qquad \text{S.34}$$

$\mathrm{\beta_{CCS}}$: cost of low-carbon electricity (CCS electricity), $\$/\mathrm{GJ}$

$\mathrm{\beta_{PSA}}$: cost of electricity from [NGCC-PSA-storage] (the value can change based on the carbon price and the amount of captured CO_2), $\$/\mathrm{GJ}$

$\mathrm{\beta_{NGCC}}$: cost of electricity from NGCC, $\$/\mathrm{GJ}$

$\mathrm{\beta_{MEA}}$: cost of electricity from [NGCC-MEA-storage] (the value can change based on the carbon price and the amount of captured CO_2), $\$/\mathrm{GJ}$

$\mathrm{\delta_{CO_2}}$: cost of the CO_2 transportation and storage in underground (obtained in IECM, assuming a 50 km pipeline is used for transportation), $\$/\mathrm{ton_{CO\,_2s}}$

$\mathrm{F_{MEA,CO_{2s}}}$: cost of electricity from [NGCC-MEA-storage] (the value can change based on the carbon price and the amount of captured CO_2), $\$/\mathrm{GJ}$

S5.3. Calculation of economic factors for low-carbon heating

In this work, heating is proposed to be partially substituted by CCS electricity. As such, low-carbon heating is used in the CCU system. Herein, the economic factor for low-carbon heating is calculated as follows,

$$\beta_{\mathrm{fuel}_{\mathrm{low-C}}} = \epsilon \cdot \beta_{\mathrm{CCS}} + (1 - \epsilon)\beta_{\mathrm{fuel}} \qquad \text{S.35}$$

$$\beta_{\mathrm{steam}_{\mathrm{low-C}}} = \varepsilon \cdot \beta_{\mathrm{CCS}} + (1 - \varepsilon)\beta_{\mathrm{steam}} \qquad \text{S.36}$$

Where,

$\beta_{\mathrm{fuel}_{\mathrm{low-C}}}$: economic factor for low-carbon heating (partially by CCS electricity and partially by fuel gas), ton/GJ

β_{fuel}: economic factor for heating by fuel gas, ton/GJ

$\beta_{\mathrm{steam}_{\mathrm{low-C}}}$: economic factor for low-carbon heating (partially by CCS electricity and partially by steam), ton/GJ

β_{steam}: economic factor for heating by steam, ton/GJ

S5.4. Calculation of economic factors involving with carbon tax.

The economic factors contain two parts: original prices and carbon tax.

$$\beta_{\mathrm{r}} = \beta_{\mathrm{r},0} + \alpha_{\mathrm{r}} \cdot \gamma_{\mathrm{CO_2}} \qquad \text{S.37}$$

$$\beta_{\mathrm{u}} = \beta_{\mathrm{u},0} + \alpha_{\mathrm{u}} \cdot \gamma_{\mathrm{CO_2}} \qquad \text{S.38}$$

$$\beta_{\mathrm{p}} = \beta_{\mathrm{p},0} + \alpha_{\mathrm{p}} \cdot \gamma_{\mathrm{CO_2}} \qquad \text{S.39}$$

Where

β	Economic factors, $\$/\mathrm{ton_r}$
α	Emission factors, $\mathrm{ton_{CO_2}}/\mathrm{ton_p}$
γ_{CO_2}	Carbon price, $\$/\mathrm{ton_{CO_2}}$
Subscript	
i	Notation for sub-systems
r	Notation for raw materials (natural gas, process water, MEA, etc.)

u	Notation for utilities (steam, fuel gas, electricity, cooling, etc.)
p	Notation for products (gasoline, diesel, methanol, etc.)

S5.5. Data for economic factors

For the key materials (NG, methanol, gasoline, diesel), we use the prices data in the first half of 2021. Due to the EU energy crisis in the second half of 2021, the prices for all petrol-products dramatically surge in different speeds [FT], so the very latest price data may cause bias in the economic analysis.

Table S4. Economic factors for materials ($\beta_{r,0}$ or $\beta_{p,0}$), utilities ($\beta_{u,0}$) and CO_2 storage (δ_{CO_2})

	Economic factors [\$/ ton]	Unit	source
Natural gas	475.4	$\$/\text{ton}_{\text{NG}}$	1)
Process water	0.036	$\$/\text{ton}_{\text{water}}$	2)
Methanol	475.6	$\$/\text{ton}_{\text{MEOH}}$	3)
Gasoline	2254.8	$\$/\text{ton}_{\text{gasoline}}$	4)
Diesel	1808.6	$\$/\text{ton}_{\text{diesel}}$	4)
MEA	1100.0	$\$/\text{ton}_{\text{MEA}}$	5)
Ethanol	705.7	$\$/\text{ton}_{\text{EtOH}}$	6)
C2-C4	1067.2	$\$/\text{ton}_{\text{C3}}$	6)
Electricity	41.34	$\$/\text{GJ}_{\text{NGCC}}$	1)
Fuel gas	9.76	$\$/\text{GJ}_{\text{fuel-gas}}$	1)
Steam	15.35	$\$/\text{GJ}_{\text{steam}}$	7)
Cooling water	0.029	$\$/\text{ton}_{\text{water}}$	2)
Cooling utility	0.43	$\$/\text{GJ}_{\text{cooling}}$	8)
CO_2 storage	5.56	$\$/\text{ton}_{\text{CO}_2\text{s}}$	9)

1) Eurostat. Choose the prices for EU in the first half 2021.[23]
2) Boulamanti *et al.* [24]

3) Methanex. Choose the prices for EU in April 2021.[25]
4) European Commission – Weekly Oil Bulletin. Choose the prices for EU in April 2021.[26]
5) Brandl *et al*.[27]
6) ICIS 2019 EU.[28]
7) TLV.[29]
8) The cost of cooling is calculated by cooling water emission factor times its required amount (based on $\Delta T = 20℃$, heat transfer efficiency $\eta = 0.8$).
9) δ_{CO_2}: cost of the CO_2 transportation and storage in underground is obtained in IECM (assuming a 50 km pipeline is used for transportation).[1]

S6. Single-objective optimization (LCA) of the industrial park

S6.1. Optimal operating condition by single-objective optimization

Table S5. Initial guess and optimal values (by GA) for decision variables for single objective optimization.

	Decision variables θ	Unit	Initial (base case)	Optimal	Decision index
MEA	r_{CO_2}	-	0.775	0.933	(1)
1st PSA	P_{L1}	bar	0.0075	0.007	(2)
	P_{I1}	bar	0.285	0.406	(3)
	v_{feed1}	m s^{-1}	1.05	0.614	(4)
	t_{ads1}	s	60	68.789	(5)
	t_{bd1}	s	115	32.515	(6)
	t_{evac1}	s	115	183.637	(7)
2nd PSA	P_{L2}	bar	0.0275	0.014	(8)
	P_{I2}	bar	0.285	0.170	(9)
	v_{feed2}	m s^{-1}	1.05	0.534	(10)
	t_{ads2}	s	60	59.411	(11)
	t_{bd2}	s	115	44.544	(12)
	t_{evac2}	s	115	178.820	(13)
CO_2 to FT	z_{FT}	-	0.75	0.027	(14)
FT	T_{FT}	°C	240	248	(15)
	P_{FT}	bar	32.5	25.904	(16)
	$tray_{FT}$	-	55	62	(17)
	T_{ref1}	°C	875	876	(18)
	P_{ref1}	bar	5	5.073	(19)
	S_{purge}	-	0.1005	0.045	(20)
	Re_{FT}	-	0.5	0.573	(21)
MS	F_{NG}/F_{CO_2}	-	2.85	3.498	(22)
	T_{MS}	°C	200	204	(23)
	P_{MS}	bar	65	69.542	(24)
	$Tray_{MS}$	-	55	46	(25)
	T_{ref2}	°C	900	933	(26)
	P_{ref2}	bar	5	6.224	(27)
Heating utility	$Frac_{fuel_{ele-CCS}}$	-	0.2	0.997	(28)
	$Frac_{steam_{ele-CCS}}$	-	0.2	0.956	(29)

S6.2. Simulation by surrogates *vs.* rigorous process models

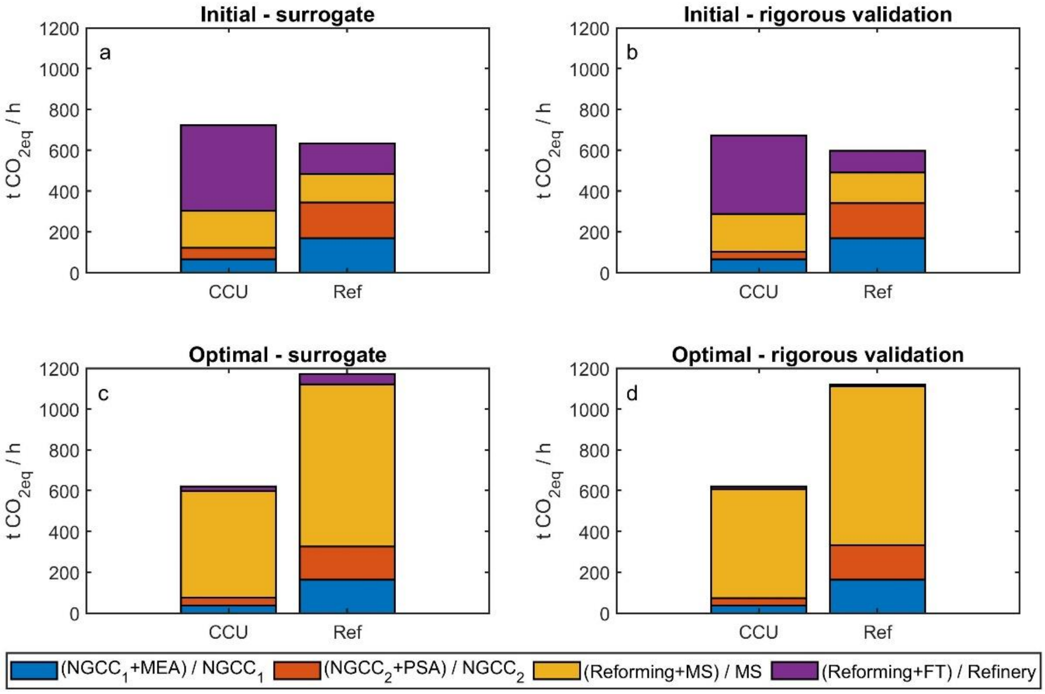

Figure S10. Validation of surrogate models by rigorous simulation for the industrial park regarding: (a) initial operating condition based on surrogates; (b) initial operating condition based on rigorous process models; (c) optimal operating condition based on surrogates; (d) optimal operating condition based on rigorous process models. For the legends: left of '/' for CCU system, right of '/' for the reference system.

S6.3. Scenario analysis for heating utility substituted by low-carbon electricity

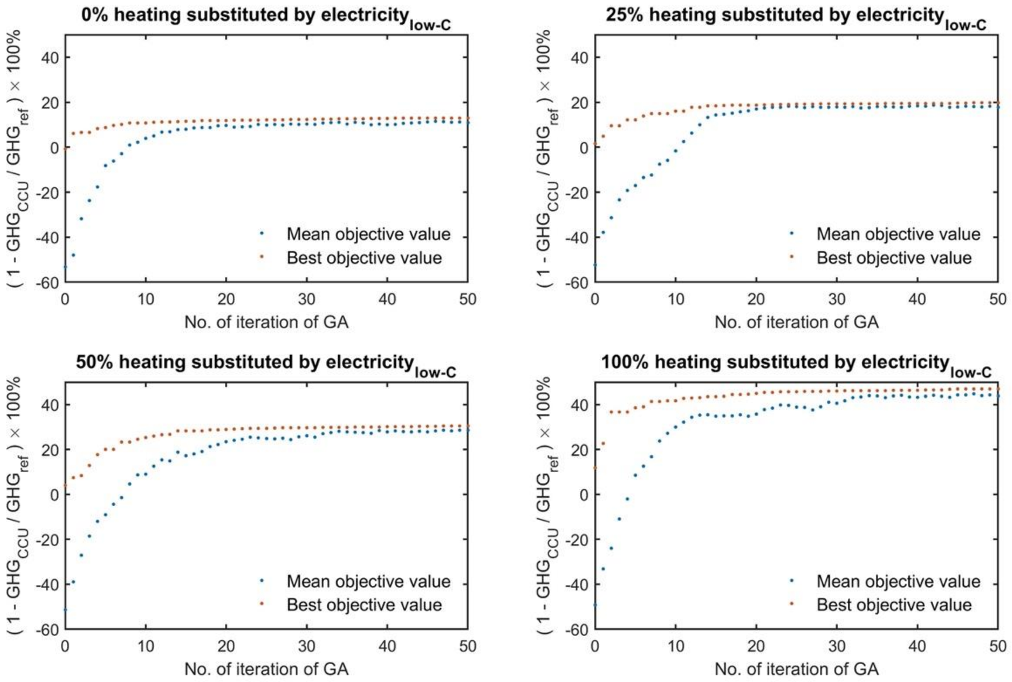

Figure S11. Scenario analysis for the optimization progress, regarding 10%, 25%, 50% and 100% heating utility is substituted by low-carbon electricity.

Table S6. Scenario analysis for optimal values of decision variables, regarding maximum 10%, 25%, 50% and 100% heating utility is substituted by electricity.

			Max heating percentage substituted by CCS-elec			
	design variables	Unit	1	0.5	0.25	0
MEA	r_{CO_2}	-	0.933	0.935	0.917	0.925
1st PSA	P_{L1}	bar	0.007	0.008	0.006	0.006
	P_{I1}	bar	0.406	0.375	0.447	0.203
	v_{feed1}	m/s	0.614	0.614	1.265	0.857
	t_{ads1}	s	68.789	80.648	51.744	69.800
	t_{bd1}	s	32.515	54.996	50.743	42.274
	t_{evac1}	s	183.637	179.226	194.448	190.152
2nd PSA	P_{L2}	bar	0.014	0.011	0.011	0.019
	P_{I2}	bar	0.170	0.266	0.432	0.267
	v_{feed2}	m/s	0.534	0.917	0.917	0.316
	t_{ads2}	s	59.411	46.559	59.411	60.379
	t_{bd2}	s	44.544	36.050	35.890	82.815
	t_{evac2}	s	178.820	178.820	191.707	176.463
CO_2 to FT	z_{FT}	-	0.027	0.027	0.046	0.027
FT	T_{FT}	℃	247.886	263.910	254.435	257.929
	P_{FT}	bar	25.904	17.334	46.535	42.624
	$tray_{FT}$	-	62	52	52	52
	T_{ref1}	℃	876.081	876.081	774.820	858.981
	P_{ref1}	bar	5.073	5.130	4.730	3.129
	S_{purge}	-	0.045	0.069	0.194	0.102
	Re_{FT}	-	0.573	0.828	0.660	0.468
MEOH	F_{NG}/F_{CO}	-	3.498	3.643	3.656	3.656
	T_{MS}	℃	204.318	198.258	187.149	189.011
	P_{MS}	bar	69.542	78.283	75.294	77.341
	$Tray_{MS}$	-	46	61	60	64
	T_{ref2}	℃	933.319	864.478	913.001	876.951
	P_{ref2}	bar	6.224	4.615	5.474	5.176
Heating utility	$Frac_{fuel_{ele-CCS}}$	-	0.997	0.498	0.250	0.000
	$Frac_{steam_{ele-CCS}}$	-	0.956	0.496	0.223	0.000

S7. Multi-objective (LCA-Economic) optimization of the industrial park

S7.1. Optimal values for decision carbon @ Carbon price = 0

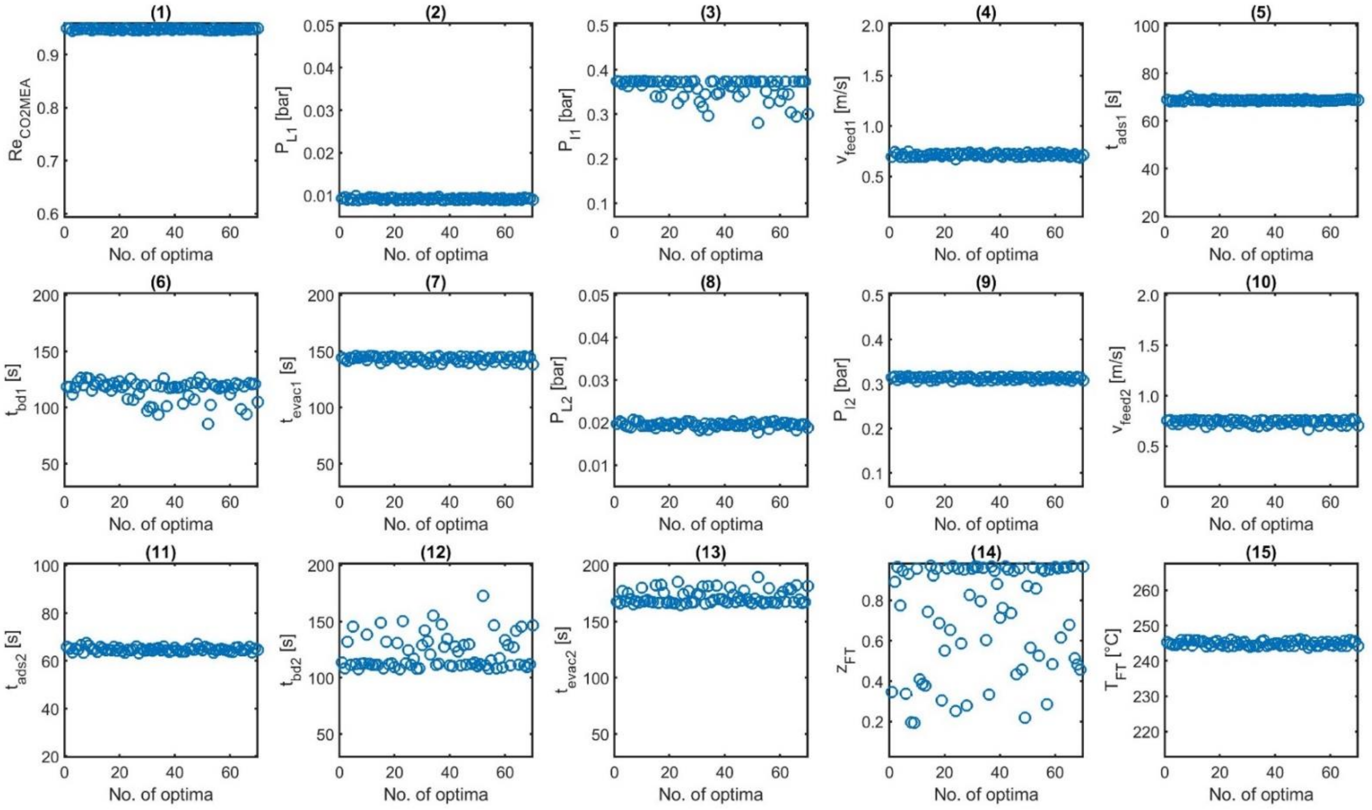

Figure S12. Optimal values of decision variables $x_1 \sim x_{15}$ after multi-objective optimization @ $C_{tax} = 0$ \$/ton-CO$_2$ (corresponding to the Pareto front in Figure 8).

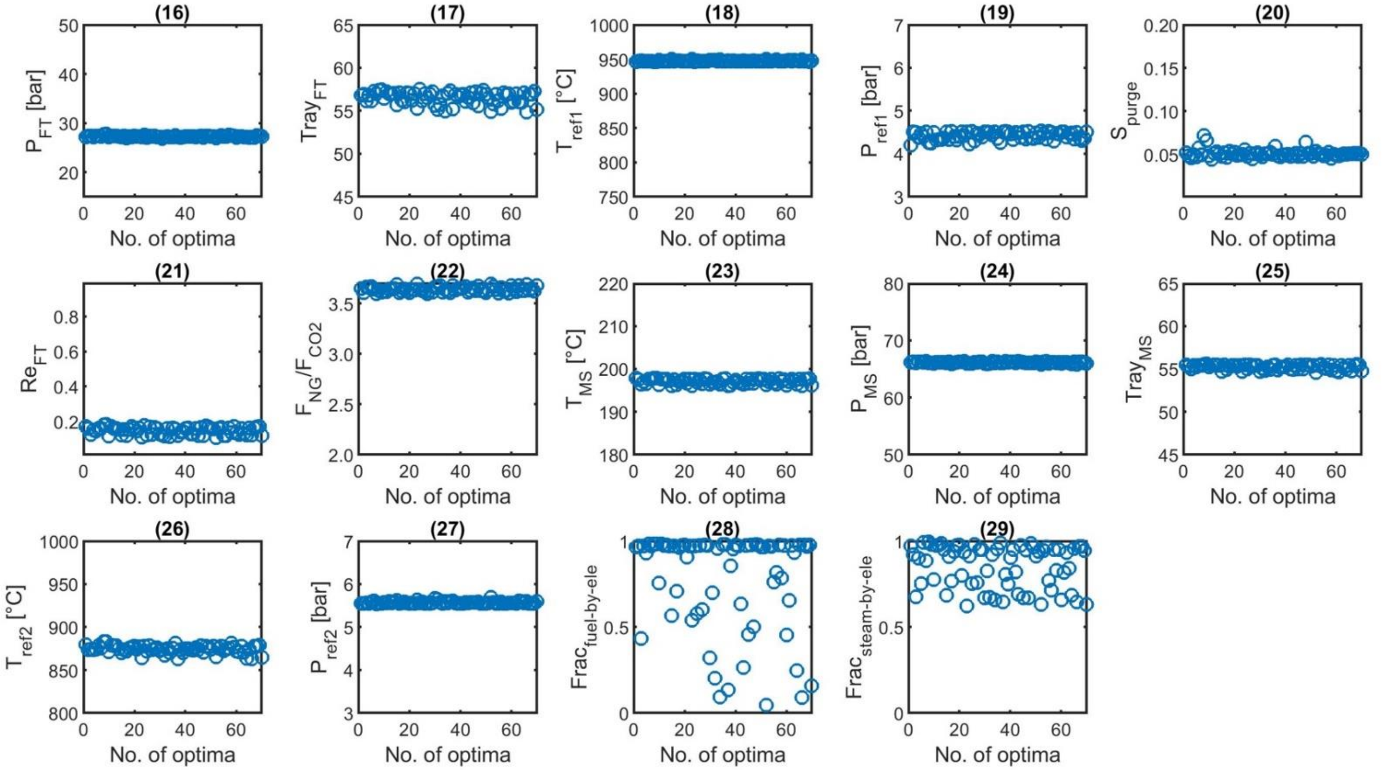

Figure S13. Optimal values of decision variables x_{16}~x_{29} after multi-objective optimization @ $C_{tax} = 0$ \$/ton-CO$_2$ (corresponding to the Pareto front in Figure 8).

S7.2. Evaluation of utilities

As indicated by the single-objective optimization, the heating utility is accounted for the biggest role in the GHG emissions. Herein, we once again check the influence of optimized utility on both economic aspects and GHG emissions. NSGA-II promotes low-carbon heating. On the one hand, switching to the low-carbon electricity increases the energy cost, by 25% for electricity and by average 337% for fuel-gas heating as well as 201% for steam heating. On the other hand, switching to the low-carbon electricity dramatically reduces the GHG emissions, by 76% for electricity and by 52% for fuel-gas heating as well as average 57% for steam heating.

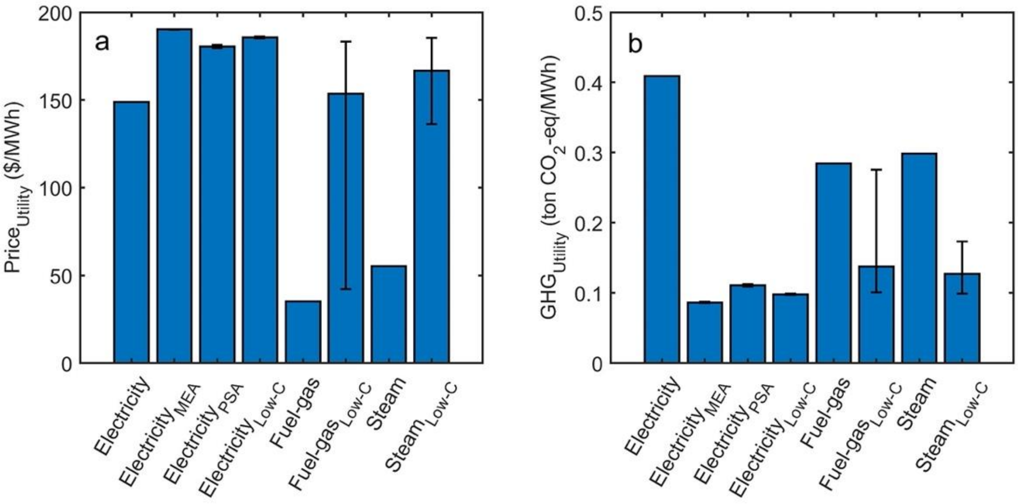

Figure S14 (a) Price of utilities. (b) GHG emissions of utilities. Clarification for the x-axis label - (1) $Electricity$: NG-based power plant with direct emissions; (2) $Electricity_{MEA}$: NG-based power plant coupled with MEA; (3) $Electricity_{PSA}$: NG-based power plant coupled with PSA; (4) $Electricity_{Low-C}$: low-carbon electricity, which is approximated by the average value between $Electricity_{MEA}$ and $Electricity_{PSA}$ (the cost of CO_2 storage is included); (5) $Fuel\text{-}gas$: heating provided by fuel gas; (6) $Fuel\text{-}gas_{Low-C}$: fuel-gas heating partially substituted by low-carbon electricity; (7) $Steam$: heating provided by steam; (8) $Steam_{Low-C}$: steam heating partially substituted by low-carbon electricity.

S7.3. Robustness of optimal solutions

To check whether the best solutions found in our case are robust or not, we evaluate two extreme scenarios regarding the selection of utilization pathways – fully employing either FT or MS. As shown in Figure S15, either way does not deliver better solutions than the found solution found by NSGA-II. On the one hand, the CO_2 utilization *via* entirely FT tends to bring in a higher profit, but the potential for GHG emissions reduction is limited to 20%. On the other hand, fully MS can enhance GHG emissions reduction to 46% but dramatically lose the economic advantage compared to the original solution found by NSGA-II.

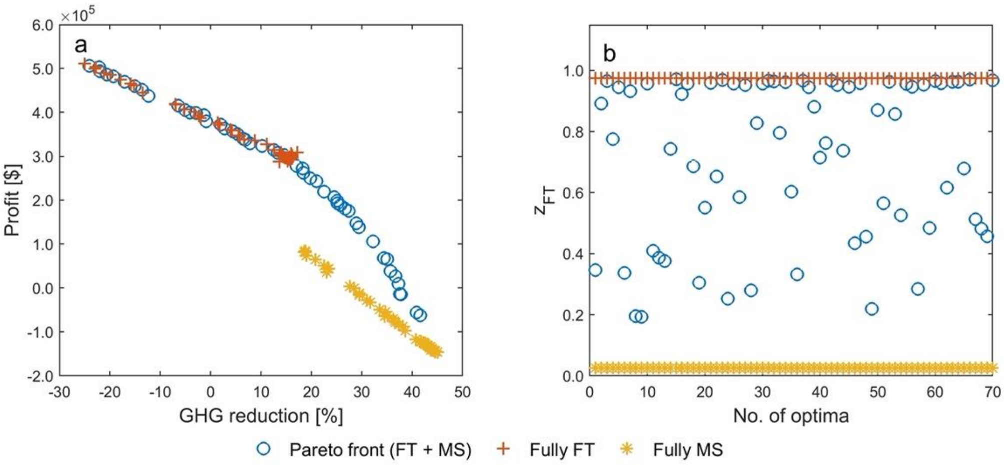

Figure S15. Influence of different utilization pathways: (a) Trade-off between profit and GHG reduction for the industrial park. (b) the fraction of CO_2 utilization via FT (values of other operating conditions keep the same).

Similarly, we evaluate another extreme scenario, where the heating is fully substituted by low-carbon electricity. As shown in Figure S16, such a complete substitution brings in minor improvement on GHG reduction but significantly sacrifices the economic gain.

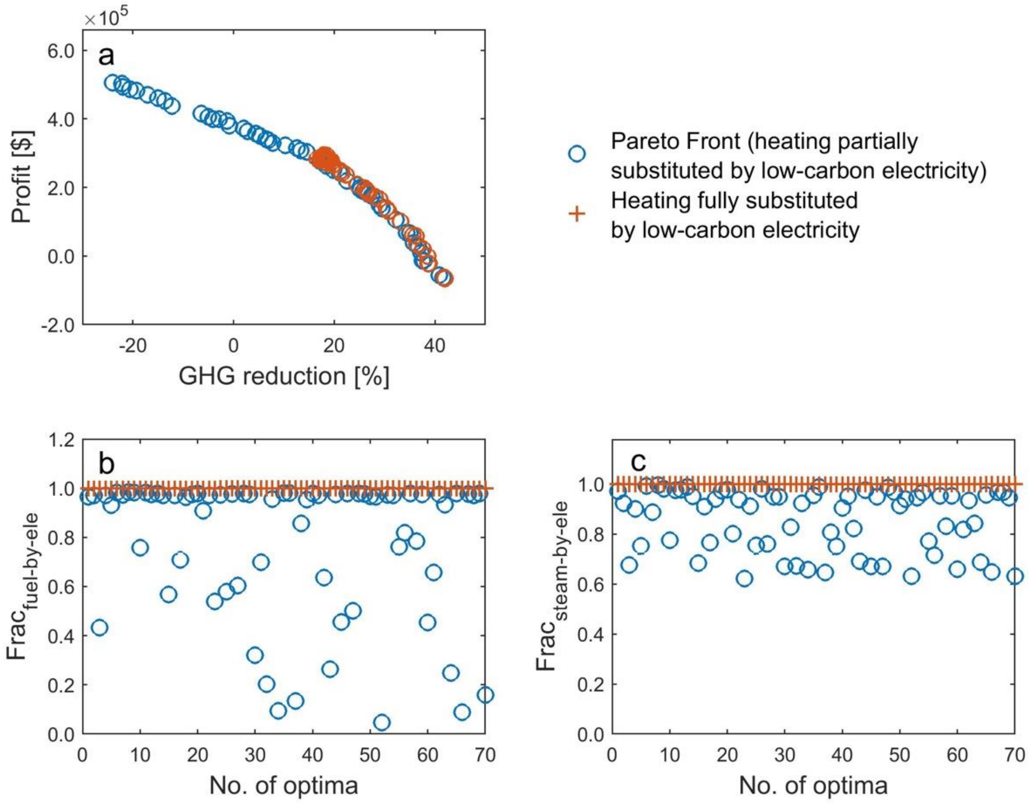

Figure S16. Influence of the heating fully substituted by low-carbon electricity: (a) trade-off between profit and GHG reduction for the industrial park; (b) the fraction of fuel-gas heating substituted by low-carbon electricity; (c) the fraction of steam heating substituted by low-carbon electricity (values of other operating conditions keep the same).

Reference

1. IECM, Integrated Environmental Control Model (IECM) Version 11.4 (Carnegie Mellon University), https://www.cmu.edu/epp/iecm/index.html, accessed: 2020-08-01.
2. Z. Hao, C. Zhang and A. Lapkin, Efficient Surrogates Construction of Chemical Processes: Case studies on Pressure Swing Adsorption and Gas-to-Liquids. *ChemRxiv*, 2021.
3. R. Haghpanah, A. Majumder, R. Nilam, A. Rajendran, S. Farooq, I. A. Karimi and M. Amanullah, *Ind Eng Chem Res.*, 2013, **52**, 4249-4265.
4. Z. Hao, A. Caspari, A. M. Schweidtmann, Y. Vaupel, A. A. Lapkin and A. Mhamdi, *Chem Eng J.*, 2021, **423**, 130248.
5. K.-S. Ha, J. W. Bae, K.-J. Woo and K.-W. Jun, *Environ Sci Technol.*, 2010, **44**, 1412-1417.

6. M. E. Dry, *Catal Today*, 2002, **71**, 227-241.
7. J. R. van Ommen and J. Grievink, in *Biomass as a Sustainable Energy Source for the Future*, 2014, pp. 525-546.
8. Y. H. Kim, K.-W. Jun, H. Joo, C. Han and I. K. Song, *Chem Eng J.*, 2009, **155**, 427-432.
9. C.-J. Lee, Y. Lim, H. S. Kim and C. Han, *Ind Eng Chem Res.*, 2009, **48**, 794-800.
10. B. Bao, M. M. El-Halwagi and N. O. Elbashir, *Fuel Process Technol.*, 2010, **91**, 703-713.
11. I. C. Yates and C. N. Satterfield, *Energy Fuel*, 1991, **5**, 168-173.
12. C. G. Visconti, L. Lietti, E. Tronconi, P. Forzatti, R. Zennaro and E. Finocchio, *Appl Catal A: Gen.*, 2009, **355**, 61-68.
13. P. Kaiser, R. B. Unde, C. Kern and A. Jess, *Chem Ing Tech.*, 2013, **85**, 489-499.
14. H. Jouhara, N. Khordehgah, S. Almahmoud, B. Delpech, A. Chauhan and S. A. Tassou, *Therm Sci Eng Prog.*, 2018, **6**, 268-289.
15. P. F. Fleming and B. J. Church, in *Plant Engineer's Reference Book (Second Edition)*, ed. D. A. Snow, Butterworth-Heinemann, Oxford, 2002, pp. 13-11 ~ 13-35.
16. AspenTech, *Aspen Plus Methanol Synthesis Model*, 2018. The methanol synthesis model can be downloaded from esupport.aspentech.com. Alternatively, for Aspen Plus V11 and higher version, the model file can be accessed in C:\Program Files\AspenTech\Aspen Plus Vxx.x\GUI\Examples\Bulk Chemical\Methanol.
17. K. M. V. Bussche and G. F. Froment, *J Catal.*, 1996, **161**, 1-10.
18. A. Zimmermann, L. Müller, Y. Wang, T. Langhorst, J. Wunderlich, A. Marxen, K. Armstrong, G. Buchner, A. Kätelhön and M. Bachmann, *Techno-Economic Assessment & Life Cycle Assessment Guidelines for CO2 Utilization (Version 1.1)*, 2020.
19. D. Weisser, *Energy*, 2007, **32**, 1543-1559.
20. K. Roh, A. S. Al-Hunaidy, H. Imran and J. H. Lee, *AIChE J.*, 2019, **65**, e16580.
21. R. M. Cuéllar-Franca, P. García-Gutiérrez, S. F. R. Taylor, C. Hardacre and A. Azapagic, *Faraday Discuss*, 2016, **192**, 283-301.
22. I. Muñoz, K. Flury, N. Jungbluth, G. Rigarlsford, L. M. i Canals and H. King, *The Int J Life Cycle Ass.*, 2014, **19**, 109-119.
23. Eurostat, Natural gas price statistics, https://ec.europa.eu/eurostat/statistics-explained/index.php?title=Natural_gas_price_statistics#Natural_gas_prices_for_non-household_consumers, accessed: 2021-08-01.
24. A. Boulamanti and J. A. Moya, *Renew Sust Energy Reviews*, 2017, **68**, 1205-1212.
25. Methanex, Methanex Methanol Price Sheet, https://www.methanex.com/our-business/pricing, accessed: 2021-08-01.
26. European-Commission, Weekly Oil Bulletin, https://ec.europa.eu/energy/data-analysis/weekly-oil-bulletin_en, accessed: 2021-08-01.
27. P. Brandl, M. Bui, J. P. Hallett and N. Mac Dowell, *Int J Greenh Gas Con.*, 2021, **105**, 103239.
28. ICIS, ICIS Europe Chemicals Outlooks - 2019, https://www.icis.com/explore/resources/europe-chemical-outlook-2019/, accessed: 2021-08-01.
29. TLV, Calculator: Steam Unit Cost, https://www.tlv.com/global/UK/calculator/steam-unit-cost.html. accessed: 2021-08-01.